Supplemental Data

Methyl effect on metabolism, chemical stability, and permeability profile of bioactive *N*-sulfonylhydrazones

*Jéssica de Siqueira Guedes[1,2]; Teiliane Rodrigues Carneiro[1]; Pedro de Sena Murteira Pinheiro[1]; Carlos Alberto Manssour Fraga[1,3]; Carlos Mauricio R. Sant´Anna[1,3]; Eliezer J. Barreiro[1,2]; Lídia Moreira Lima[1,2]**

TABLE OF CONTENTS

MOLECULAR MODELING

METHOD VALIDATION

HPLC CHROMATOGRAMS OF THE *N*-SULFONYLHYDRAZONES PROTOTYPES (1-4)

Metabolism study of *N*-sulfonylhydrazones prototypes (1-4)

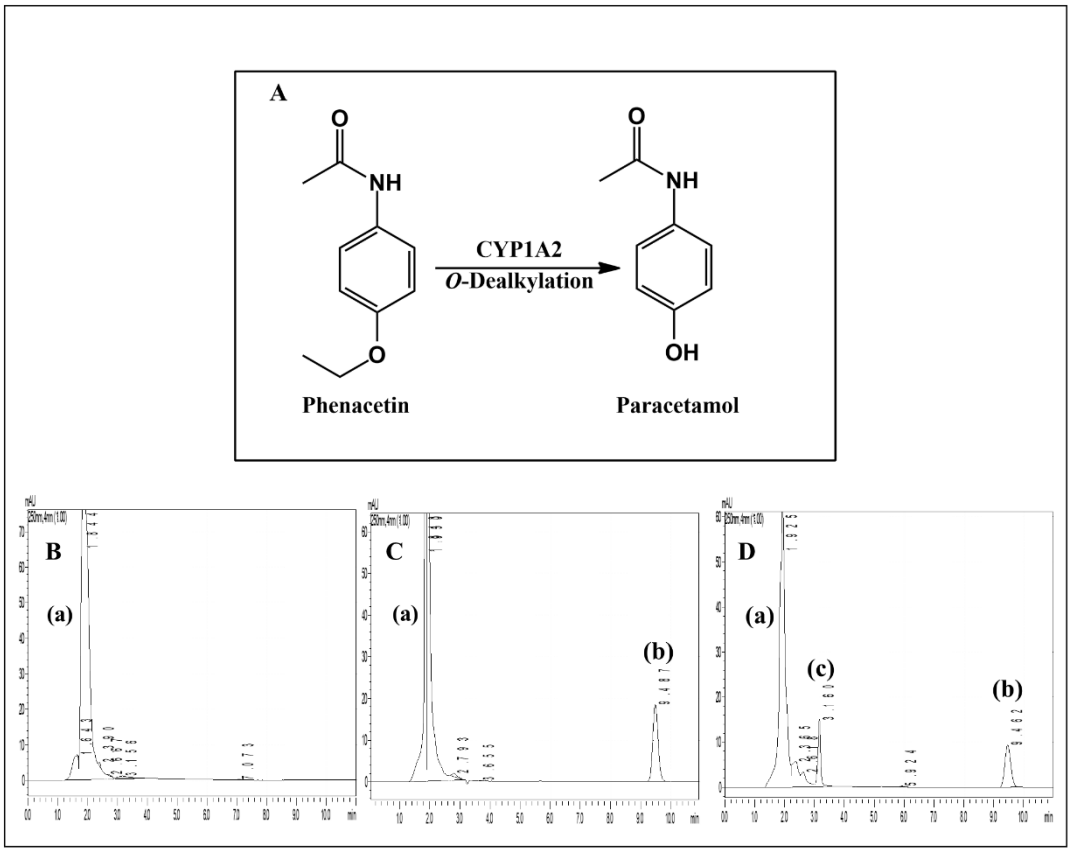

Figure S1. Validation of CYP catalytic activity in the prepared microsomal fraction using phenacetin, a known CYP1A2 substrate. Representative chromatograms of microsomal incubation of phenacetin (37 °C for 60 minutes) in the presence of an NADPH generating system. A) Biotransformation of

phenacetin into paracetamol (*O*-Dealkylation, CYP1A2). B) Representative chromatograms of the blank sample (in the absence of the subtract), emphasizing the chromatographic peak relatives to the biological matrix (**a**, R_t=1.9 min.). C) Phenacetin (**b**, Rt=9.5 min), 0 min incubation time. D) Biotransformation of phenacetin (**b**, Rt=9.5 min) into paracetamol (**c**, Rt=3.1 min), 60 min incubation time.

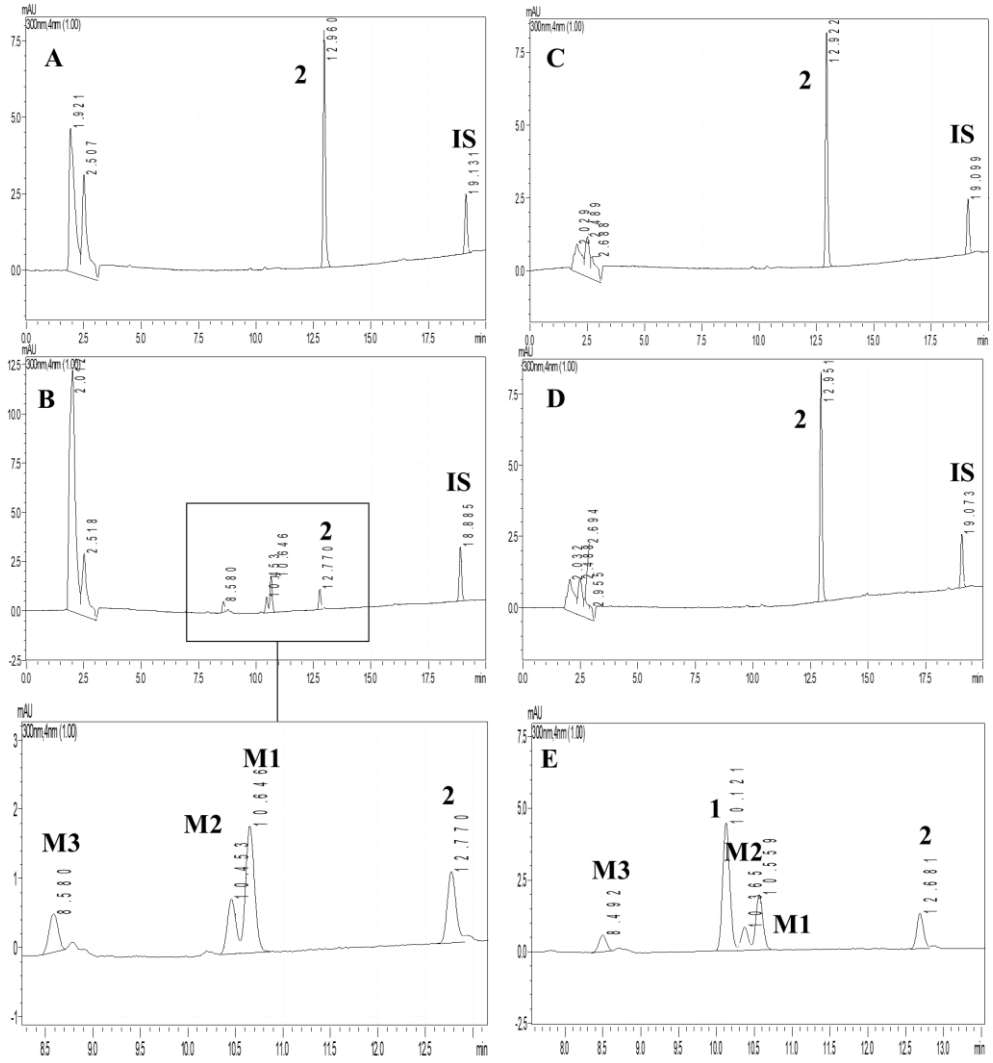

Figure S2. Representative chromatograms of microsomal metabolism of LASSBio-1772 (**2**), emphasizing the oxidative metabolites M1, M2 and M3 formed in the presence of NADPH System. IS=internal standard (biphenyl l-4-carboxylate methyl, 10 μM). A) LASSBio-1772 (**2,** R_t=12.9 min),0 min incubation time in the presence of NADPH. B) LASSBio-1772 (**2,** R_t=12.9 min), 240 min incubation time in the presence of NADPH, biotransformed in M1 (Rt = 10.6 min), M2 (Rt = 10.4 min), and M3 (Rt = 8.5 min); C) LASSBio-1772 (**2,** R_t=12.9 min), 0 min incubation time in the absence of NADPH; D) LASSBio-1772 (**2,** R_t=12.9 min), 240 min incubation time in the absence of NADPH, no metabolization. E) Co-injection of compound **1** in a metabolized sample of compound **2**, demonstrating that the M1 and M2 are not formed by *N*-demethylation since compound **1** showed a different retention time (**1**, Rt = 10.1 min) compared to M1 and M2.

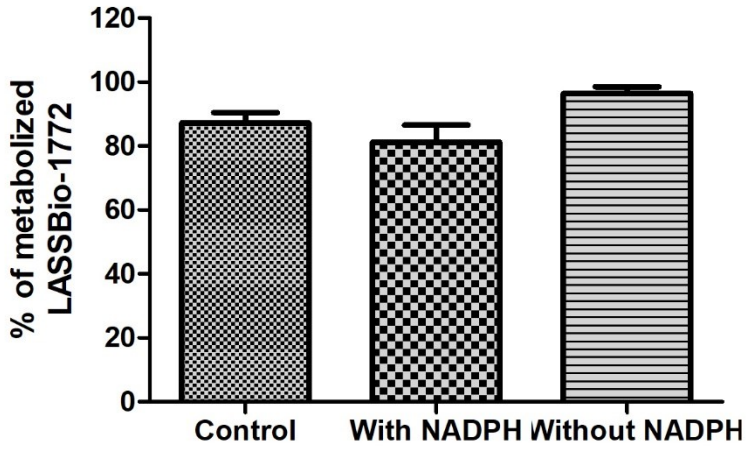

Figure S3. Alteration of in vitro hepatic metabolism of LASSBio-1772 (2), after thermal inactivation of FMO (50 °C - 1.5 minutes) in the microsomal fraction in the presence and absence of a cofactor. FMO was inactivated without NADPH. *P*-value>0.05, compared to the control (without thermal inactivation), indicating that there is no statistical difference between the groups. One-way ANOVA followed by Dunnett post-test, using the GraphPrism (version 5.0)

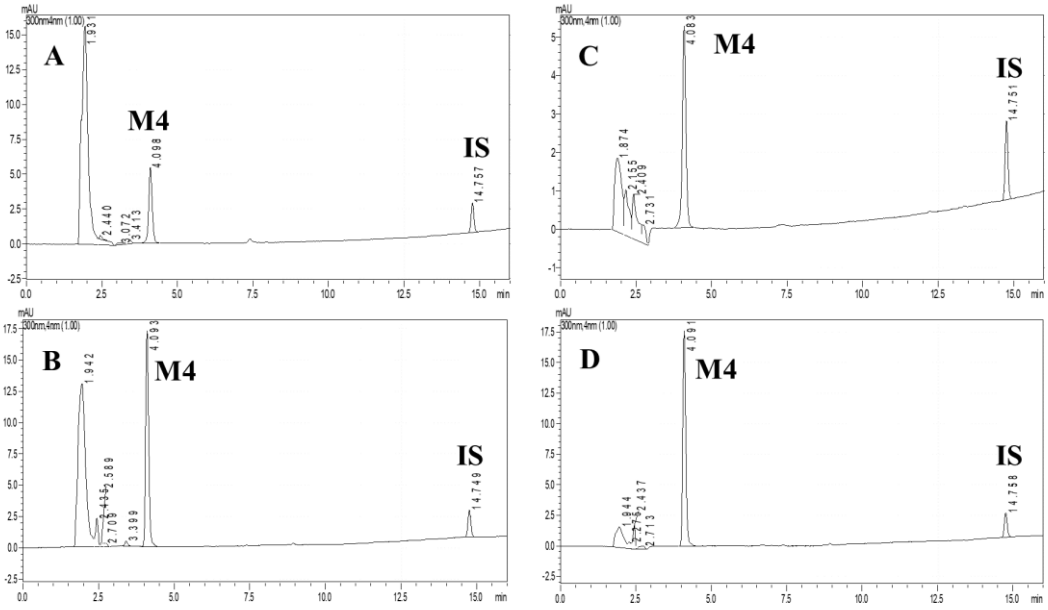

Figure S4. Representative chromatograms of spiking samples after microsomal incubation of compound **3** in the presence and absence of NADPH, at 37°C. IS=internal standard (biphenyl l-4-carboxylate methyl, 10 μM). A) M4 (Rt=4.1 min), formed in the presence of NADPH; B) **S**ample metabolized in the presence of cofactor and spiked with hydrolysis products of compound **3**; C) M4 (Rt=4.1 min), formed in the absence of NADPH; D) Sample metabolized without cofactor and spiked with hydrolysis products of compound **3**.

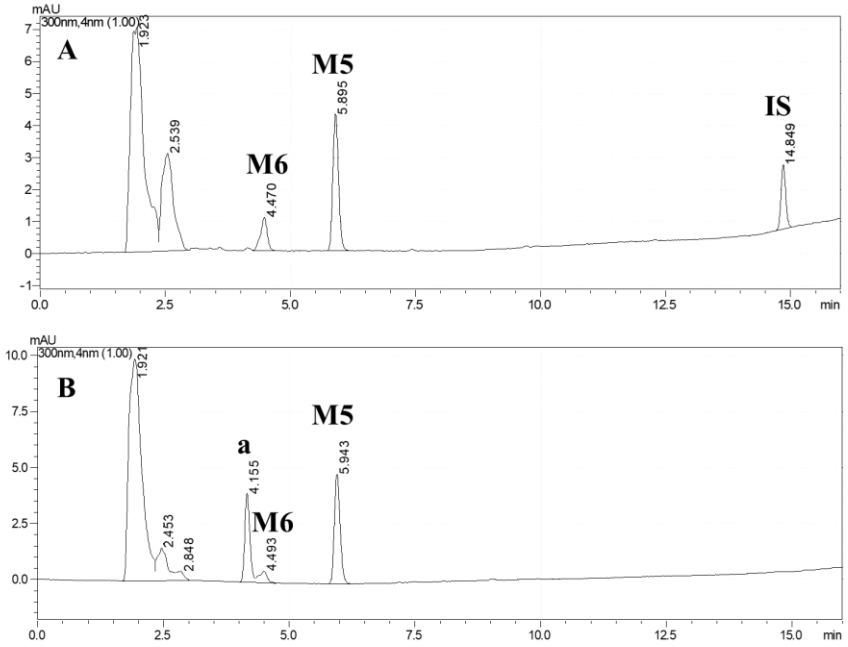

Figure S5. Representative chromatograms of spiking samples after microsomal incubation of compound **4** in the presence and absence of NADPH, at 37°C). IS=internal standard (biphenyl l-4-carboxylate methyl, 10 µM). A) M5 (Rt=5.9 min) and M6 (Rt=4.5 min), formed in the presence of NADPH; B) Sample metabolized in the presence of cofactor and co-injecting the non-*N*-methylated analog (**a**, Rt = 4.1 min) of M5.

LASSBio-1771

Considering the unexpected microsomal profile of LASSBio-1771, we hypothesized three different reasons that could explain our findings: *i*) the biotransformation products of compound **1** co-eluted with biological matrix peaks; *ii*) the developed analytical method was not able to recover and identify the formed metabolites; iii) compound **1** is a covalent ligand of some microsomal enzyme, therefore not being recovered and detected. From this perspective, we analyzed the biological matrix peaks from blank samples and compared them with previously metabolized samples of compound **1**. No increment in AUC peaks was noticed, thus the possibility of metabolites co-elution was discarded. Furthermore, to evaluate the second hypothesis, we investigate the recovery rate of the only feasible metabolite of compound **1** that could be formed

without NADPH, *i.e.,* a carboxylic acid derivative produced by cyano group hydrolysis, previously described as an *in vitro* plasma metabolite. Our results showed a recovery rate of 83% for this hydrolysis product at 10 µM, demonstrating that the developed analytical method is able to easily extract and identify it (Rt = 6.8 min) if this metabolite had been formed (Figure S6). Furthermore, taking into account the excellent recovery rate of compound **1** (range of 108-96%), we assumed that its oxidative metabolites should have a similar recovery profile, not justifying the atypical results. Among the hypotheses formulated to explain LASSBio-1771 behavior, the one that attributes to compound **1** the ability to inhibit CYP, through a covalent bond involving its nitrile subunit seems the most plausible.

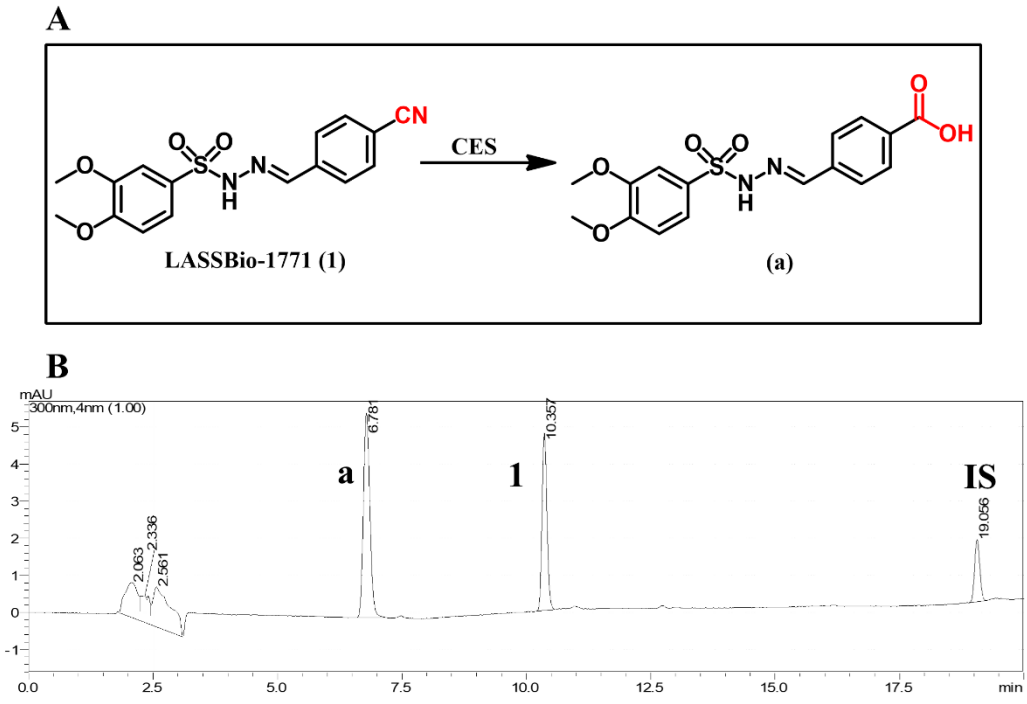

Figure S6. Recovery analysis of Compound **1** hydrolysis product (**a**) at 10 µM. A) Illustrative scheme of the cyano group hydrolysis in Compound **1**, forming the carboxylic acid derivative (**a**) by CES catalytic action. B) Representative chromatograms of recovery analysis, demonstrating that the developed analytical method can extract and identify the Compound **1** hydrolysis product (**a**, Rt = 6.8 min) if this metabolite had been formed. IS=internal standard (biphenyl l-4-carboxylate methyl, 10 µM).

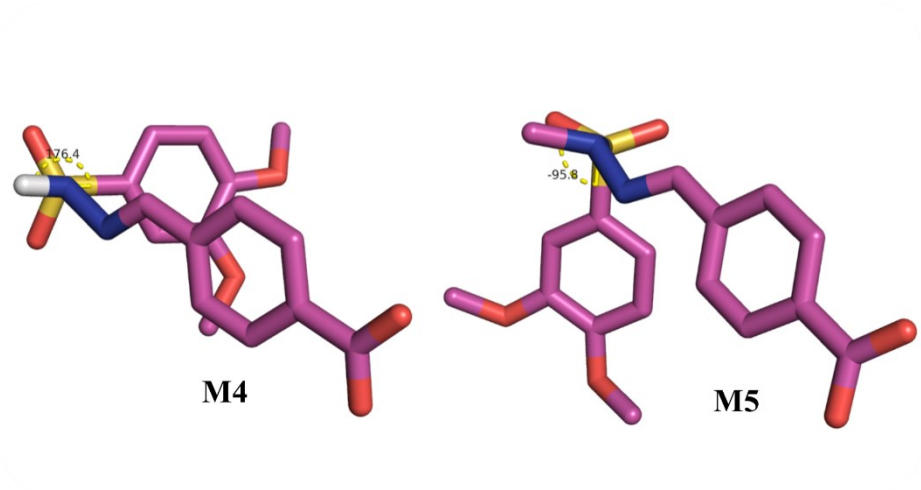

Figure S7. R-N-S-C dihedral angle comparison between the metabolites M4 from LASSBio-1773 (**3**) and M5 from LASSBio-1774 (**4**).

Chemical Stability

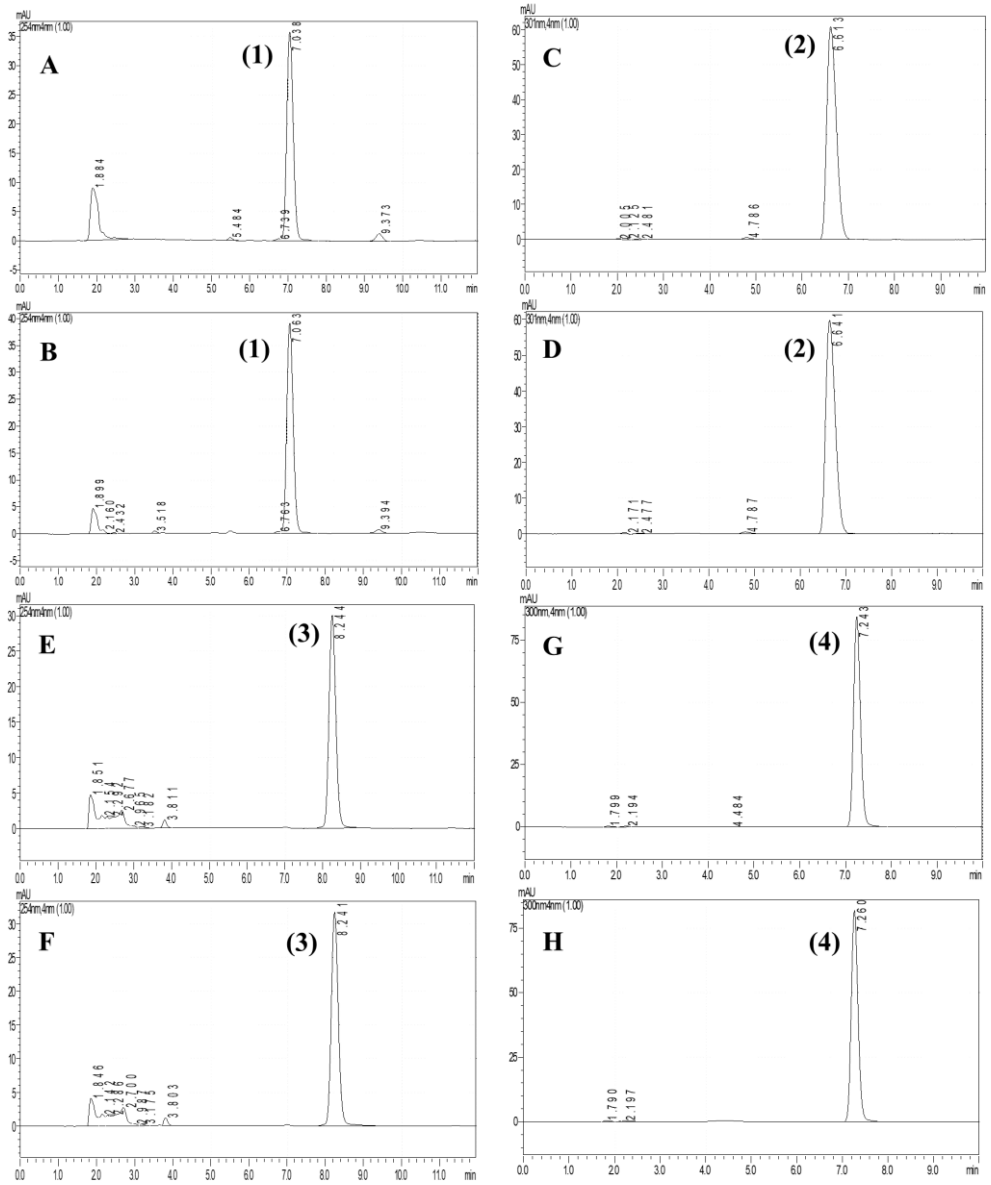

Figure S8. Representative chromatograms of chemical stability at pH 7.4 of *N*-sulfonylhydrazone prototypes (**1**-**4**). A) LASSBio-1771 (**1,** R_t=7.0 min), 0 min incubation time. B) LASSBio-1771 (**1,** R_t=7.0 min), 240 min incubation time. C) LASSBio-1772 (**2,** R_t=6.6 min), 0 min incubation time. D) LASSBio-1772 (**2,** R_t=6.6 min), 240 min incubation time. E) LASSBio-1773 (**3,** R_t=8.2 min), 0 min incubation time. F) LASSBio-1773 (**3,** R_t=8.2 min), 240 min incubation time. G) LASSBio-1774 (**4,** R_t=7.2 min), 0 min incubation time. H) LASSBio-1774 (**4,** R_t=7.2 min), 240 min incubation time.

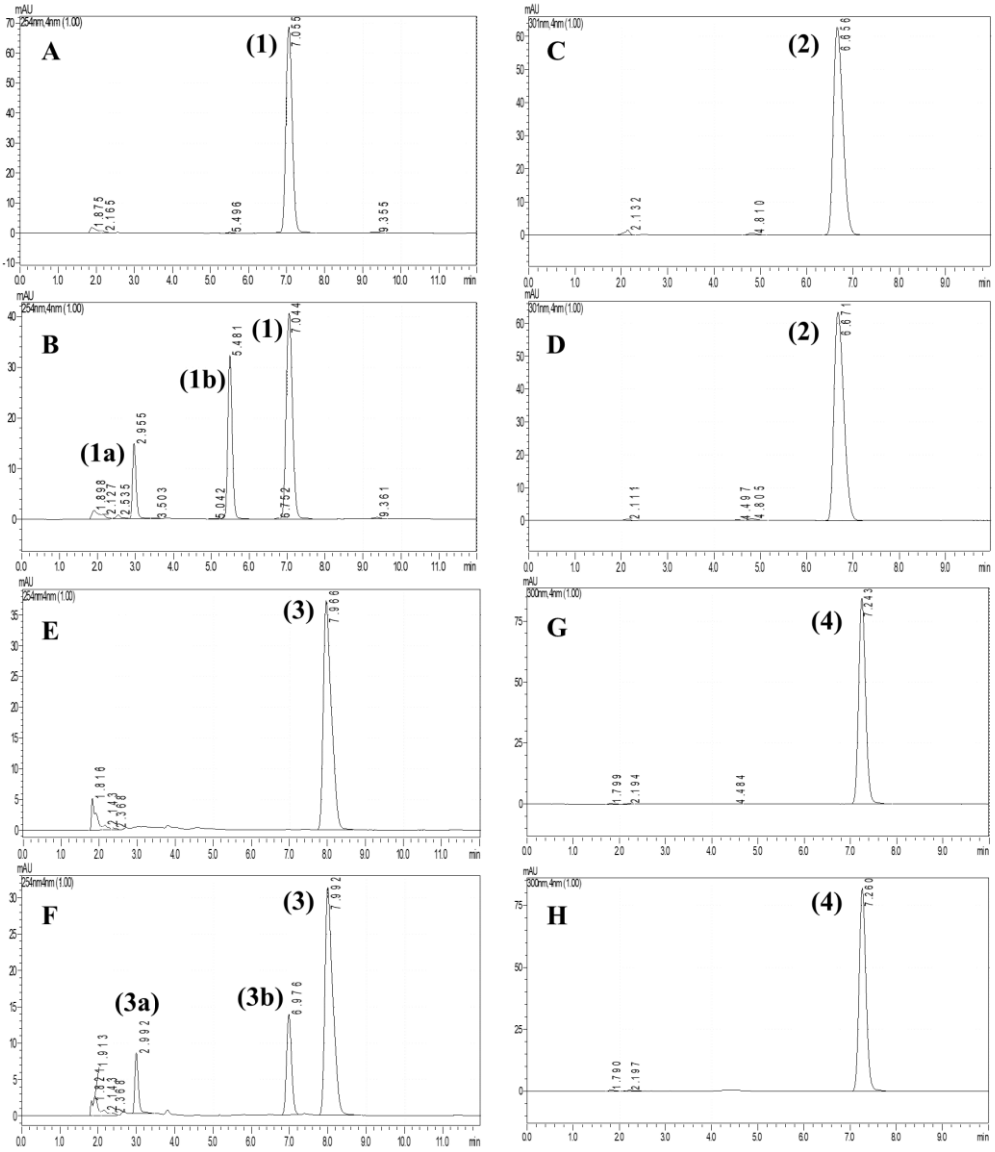

Figure S9. Representative chromatograms of chemical stability at pH 2 of *N*-sulfonylhydrazone prototypes (**1**-**4**). A) LASSBio-1771 (**1,** R_t=7.0 min), 0 min incubation time. B) LASSBio-1771 (**1,** R_t=7.0 min), 30 min incubation time, presence of hydrolysis products [(3,4-dimethoxyphenyl)sulfonyl]hydrazide (**1a**, R_t=2.9 min) and 4-formylbenzonitrile (**1b,** R_t=5.5 min). C) LASSBio-1772 (**2,** R_t=6.6 min), 0 min incubation time. D) LASSBio-1772 (**2,** R_t=6.6 min), 240 min incubation time. E) LASSBio-1773 (**3,** R_t=7.9 min), 0 min incubation time. F) LASSBio-1773 (**3,** R_t=7.9 min), 30 min incubation time, presence of hydrolysis products [(3,4-dimethoxyphenyl)sulfonyl]hydrazide (**3a**, R_t=2.9 min) and methyl-4-formylbenzoate (**3b,** R_t=6.9 min). G) LASSBio-1774 (**4,** R_t=7.2 min), 0 min incubation time. H) LASSBio-1774 (**4,** R_t=7.2 min), 240 min incubation time.

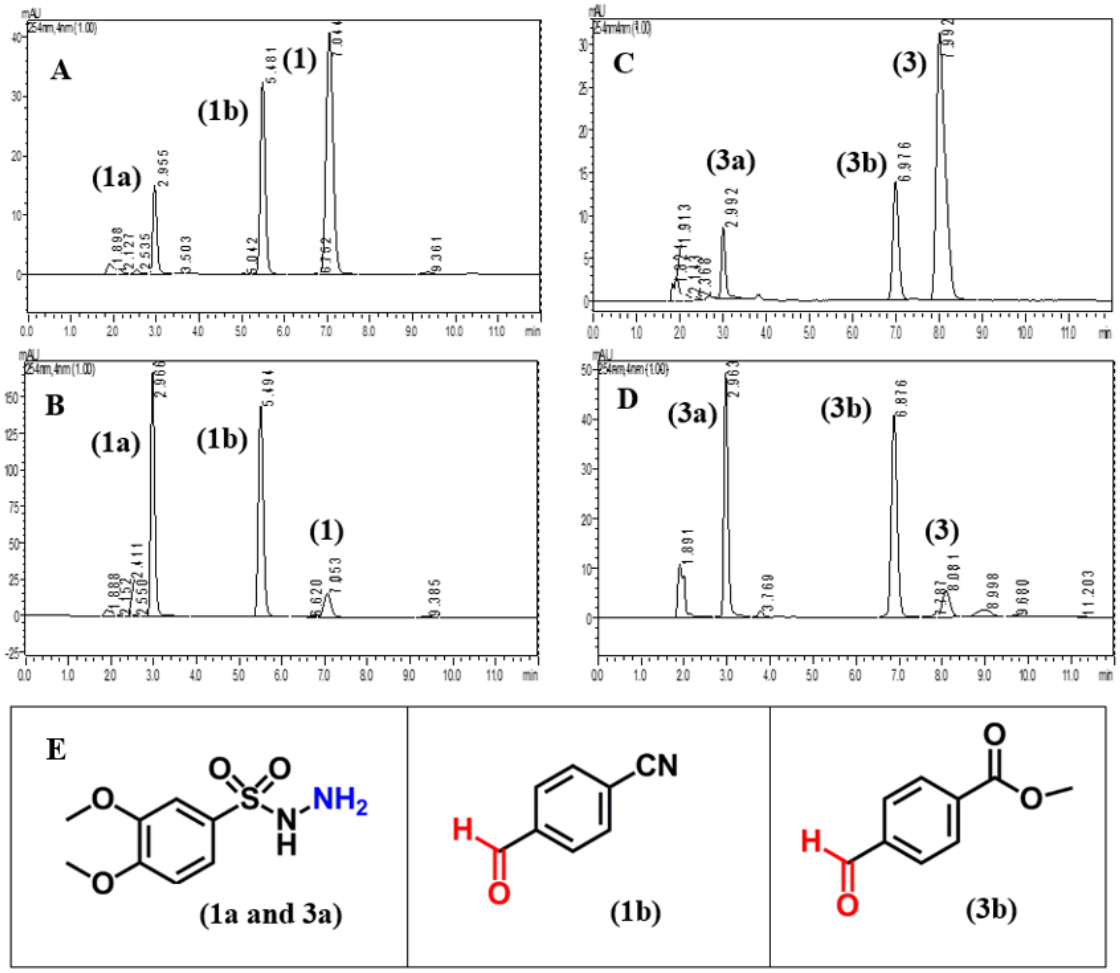

Figure S10. Representative chromatograms of spiking samples after incubation time (pH 2, at 37°C). A) LASSBio-1771 (**1,** R_t=7.0 min), 30 min incubation time, presence of hydrolysis products **1a** (R_t=2.9 min) and **1b** (R_t=5.5 min). B) samples spiked with hydrolysis products of compound **1,** [(3,4-dimethoxyphenyl)sulfonyl]hydrazide (**1a**, R_t=2.9 min) and 4-formylbenzonitrile (**1b,** R_t=5.5 min). C) LASSBio-1773 (**3,** R_t=8.0 min), 30 min incubation time, presence of hydrolysis products **3a** (R_t=2.9 min) and **3b** (R_t=6.9 min). D) samples spiked with hydrolysis products of compound **3,** [(3,4-dimethoxyphenyl)sulfonyl]hydrazide (**3a**, R_t=2.9 min) and methyl-4-formylbenzoate (**3b,** R_t=6.9 min). E) molecular structures of the hydrolysis products of Compound **1** (**1a** and **1b**), and Compound **3** (**3a** and 3**b**).

Permeability Assay

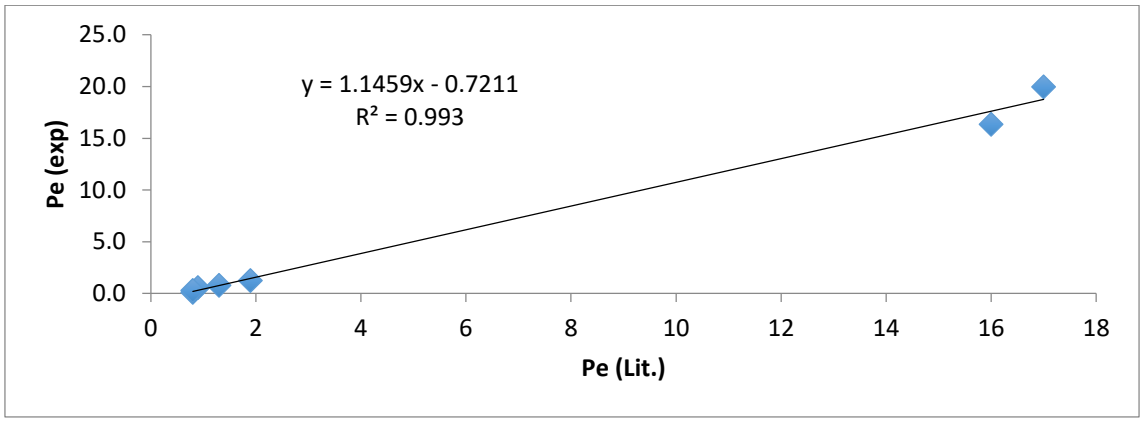

Figure S11. Prediction of brain penetration (PAMPA-BBB). Linear correlation between known permeability coefficient reported in the literature for QCs (Pe (Lit.), X-axis), and experimental values (Pe (exp), Y-axis). Experiments were performed in triplicate and at two different times (n=6). Pe values <1.57 were classified as non-permeable (BBB-), Pe values >3.86 were correlated with brain penetration ability (BBB+), and Pe values between 1.57 – 3.86 were considered as borderline

Molecular modeling

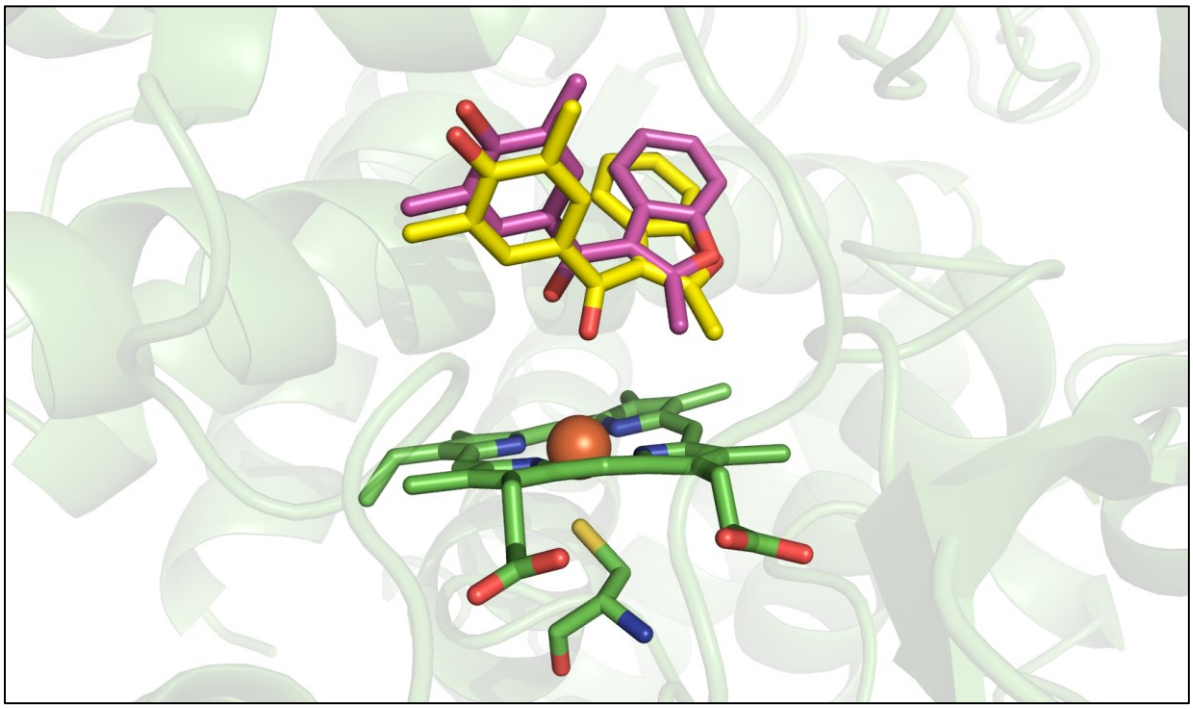

Figure S12. Comparison of the cocrystallized ligand (carbons in magenta) with the redocking analysis (carbons in yellow) using the Goldscore function (PDB: 4GQS). Analysis of CYP450 2C19 isoenzyme.

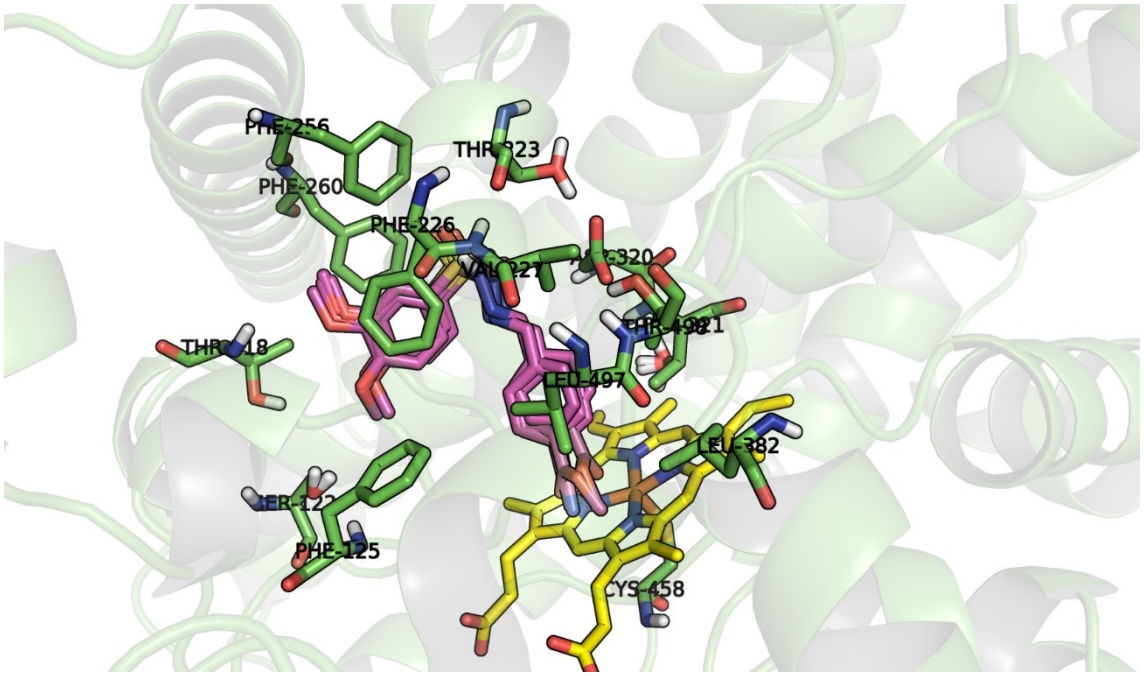

Figure S13. Comparison of the cocrystallized ligand (carbons in magenta) with the redocking analysis (carbons in yellow) using the Goldscore function (PDB 2HI4). The interaction analysis among LASSBio-1771, LASSBio-1772, LASSBio-1773, and LASSBio-1774 with CYP1A2, highlights that there are no significant differences in the interaction mode among the prototypes.

Method validation

The analytical parameters evaluated in the methods validation of metabolism study were: linearity, sensitivity, specificity, accuracy, recovery, and intra-day and inter-day precision.

The linearity was assessed considering the concentration range of 0.5 – 20 μM. The coefficient of determination (R2) was around 0.99 (R2 ~0.99) for all compounds **1-4**, and each point was analyzed in triplicate with the same concentration of the internal standard (biphenyl l-4-carboxylate methyl, 10 μM). The sensitivity was determined based on the limit of quantification (LOQ), considering a signal-to-noise ratio of at least 10. The LOQ of all prototypes (**1-4**) was 0.5 μM (Table S1).

The method specificity was defined by analyzing ten black samples co-injected with the *N*-sulfonylhydrazones prototypes (**1-4**), where no interference was noticed (Table S2). The accuracy, recovery, and intra-day and inter-day precision were determined considering the linear range of the method, using three different concentrations in triplicate (5, 10, and 15 μM) and the same concentration of the internal standard (10 μM). The accuracy was evaluated based on relative error (ER) and precision based on relative standard deviation (RSD). Our results showed that the developed

methods were accurate (RE ± 13%), precise (intra-day and inter-day precision, RSD<9%), and demonstrated excellent recovery (range 108-90%) (Table S3).

Table S1. Linearity and sensitivity data of *N*-sulfonylhydrazones prototypes (**1-4**)

Compounds	Range Concentration (µmol.L^{-1})	LOQ (µmol.L^{-1})	Linear equation	r^2
1	**0.5-20**	5	y = 0.3382x - 0.2876	0.9857
2	**0.5-20**	5	y = 0.3304x - 0.0628	0.9940
3	**0.5-20**	5	y = 0.3662x + 0.0223	0.9969
4	**0.5-20**	5	y = 0.3148x + 0.1248	0.993

Table S2. Selectivity analysis of *N*-sulfonylhydrazones prototypes (**1-4**)

Compounds	Rt analyte	Rt internal standard	Rt biological matrix
1	10.3 min	19.1 min	1.5-3 min
2	12.9 min	19.1 min	1.5-3 min
3	7.4 min	14.8 min	1.5-3 min
4	9.9 min	14.8 min	1.5-3 min

Table S3. Recovery, accuracy and precision analysis of *N*-sulfonylhydrazones prototypes (**1-4**)

Compounds	Nominal Concentration (µmol.L^{-1})	Recovery (%)	Intra-day		Inter-day	
			Precision (RSD %)	Accuracy (RE%)	Precision (RSD %)	Accuracy (RE%)
1	**5**	108.3	2.75	4.39	4.95	6.38
	10	103.9	8.62	9.35	5.47	6.67
	15	96.2	6.78	10.8	2.20	11.3
2	**5**	106.5	3.32	10.5	2.42	8.63
	10	96.4	2.32	9.26	5.87	5.54
	15	107.7	2.40	10.0	2.06	8.43
3	**5**	92.9	5.65	7.08	4.51	9.08
	10	98.1	5.42	7.88	6.49	4.88
	15	96.5	2.26	12.8	6.40	8.12
4	**5**	94.6	3.26	9.74	5.38	6.17
	10	89.6	2.93	11.4	1.57	10.4
	15	93.5	3.78	7.01	1.13	7.75

HPLC chromatograms of the N-sulfonylhydrazones prototypes (1-4)

Compound 1 – LASSBio-1771

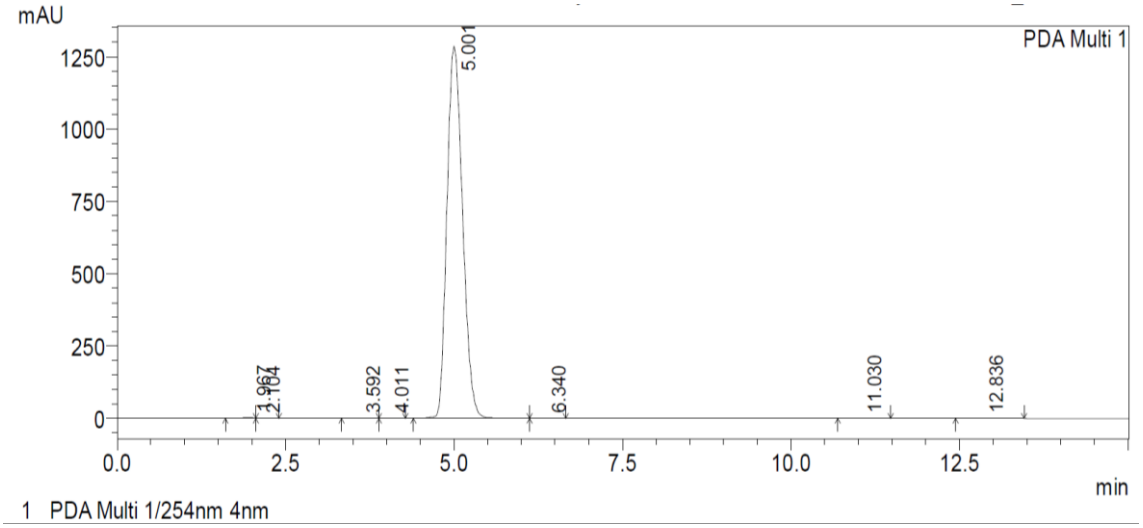

PeakTable

PDA Ch1 254nm 4nm

Peak#	Ret. Time	Area	Height	Area %	Height %
1	1.967	22638	1958	0.109	0.152
2	2.104	11064	991	0.053	0.077
3	3.592	15812	1003	0.076	0.078
4	4.011	2816	217	0.014	0.017
5	5.001	20688647	1284273	99.526	99.500
6	6.340	14281	973	0.069	0.075
7	11.030	7740	349	0.037	0.027
8	12.836	24195	966	0.116	0.075
Total		20787193	1290731	100.000	100.000

Compound 2 – LASSBio-1772

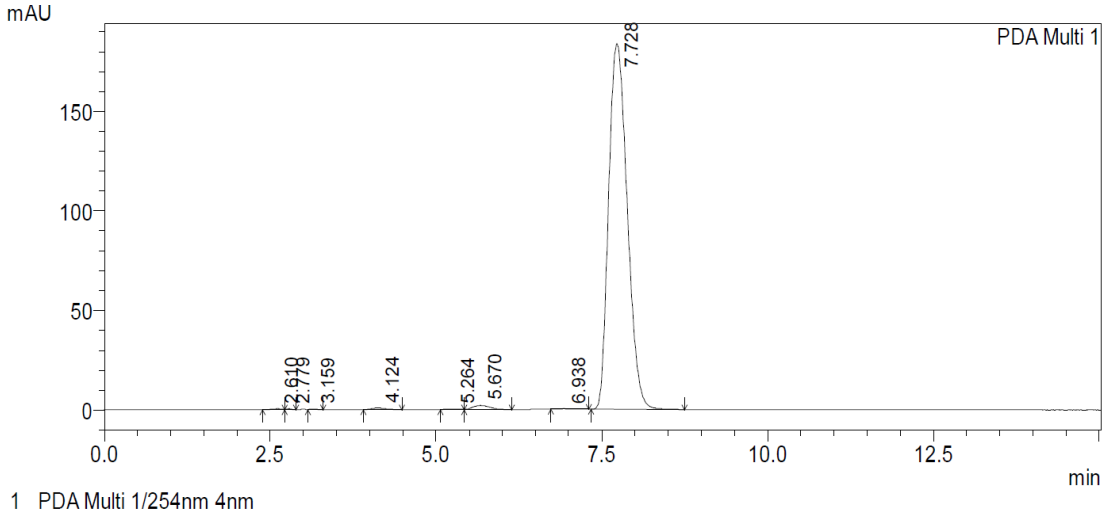

PeakTable

PDA Ch1 254nm 4nm

Peak#	Ret. Time	Area	Height	Area %	Height %
1	2.610	4075	459	0.112	0.244
2	2.779	1889	441	0.052	0.234
3	3.159	1595	277	0.044	0.148
4	4.124	10112	732	0.277	0.389
5	5.264	3712	274	0.102	0.146
6	5.670	34373	2037	0.943	1.083
7	6.938	4156	238	0.114	0.127
8	7.728	3586222	183559	98.357	97.629
Total		3646134	188016	100.000	100.000

Compound 3 – LASSBio-1773

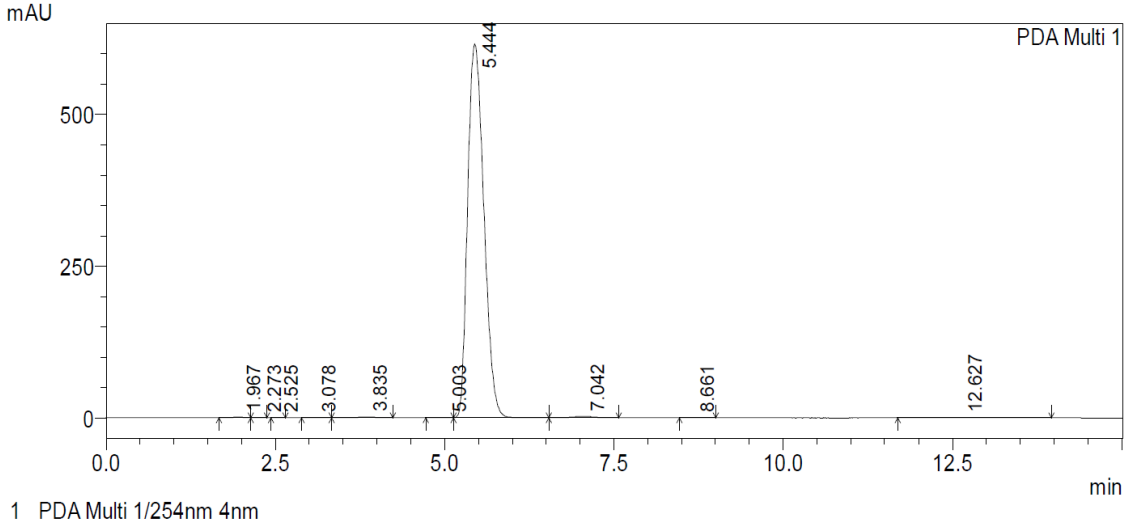

1 PDA Multi 1/254nm 4nm

PeakTable

PDA Ch1 254nm 4nm

Peak#	Ret. Time	Area	Height	Area %	Height %
1	1.967	15114	1298	0.145	0.208
2	2.273	3987	451	0.038	0.072
3	2.525	1150	185	0.011	0.030
4	3.078	2449	195	0.023	0.031
5	3.835	25307	1553	0.243	0.249
6	5.003	7400	506	0.071	0.081
7	5.444	10251153	615265	98.363	98.780
8	7.042	55105	2454	0.529	0.394
9	8.661	2465	149	0.024	0.024
10	12.627	57669	810	0.553	0.130
Total		10421799	622866	100.000	100.000

Compound 4 – LASSBio-1774

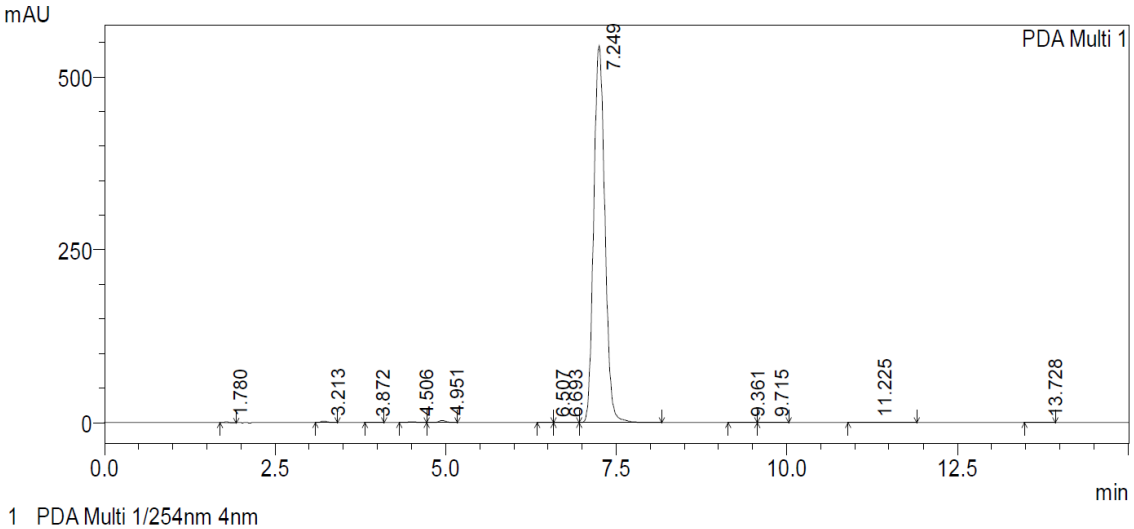

1 PDA Multi 1/254nm 4nm

PeakTable

PDA Ch1 254nm 4nm

Peak#	Ret. Time	Area	Height	Area %	Height %
1	1.780	7361	1067	0.117	0.192
2	3.213	13797	2246	0.219	0.405
3	3.872	1114	154	0.018	0.028
4	4.506	10919	1253	0.173	0.226
5	4.951	21831	2885	0.347	0.520
6	6.507	1493	165	0.024	0.030
7	6.693	5741	615	0.091	0.111
8	7.249	6210283	544650	98.640	98.260
9	9.361	4718	382	0.075	0.069
10	9.715	2648	173	0.042	0.031
11	11.225	13698	547	0.218	0.099
12	13.728	2335	158	0.037	0.028
Total		6295938	554294	100.000	100.000

Internal standard (IP) - Biphenyl l-4-carboxylate methyl

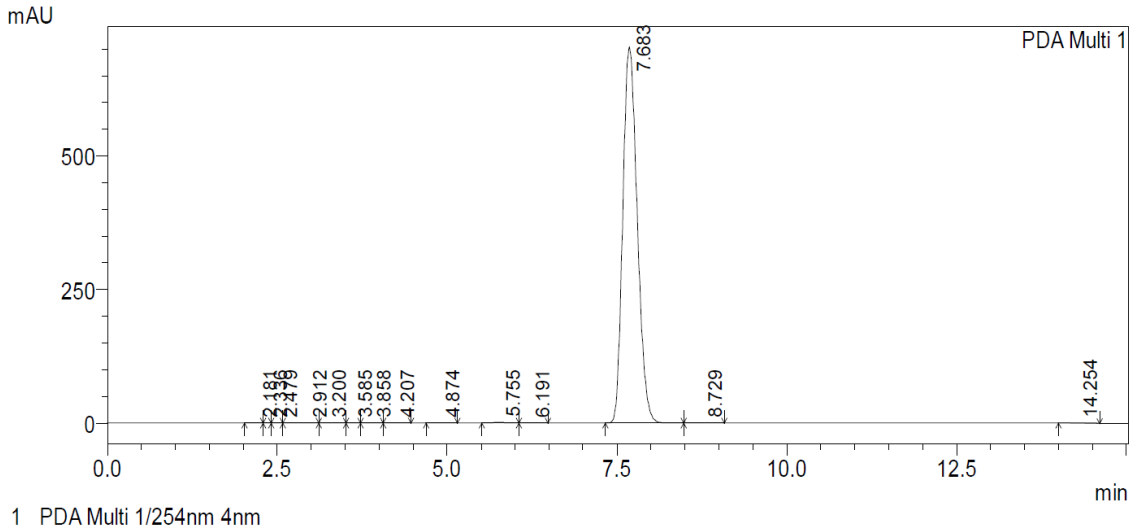

1 PDA Multi 1/254nm 4nm

PeakTable

PDA Ch1 254nm 4nm

Peak#	Ret. Time	Area	Height	Area %	Height %
1	2.181	2234	231	0.021	0.033
2	2.336	1649	243	0.016	0.034
3	2.479	2309	370	0.022	0.052
4	2.912	4920	244	0.047	0.034
5	3.200	5077	252	0.048	0.036
6	3.585	2372	229	0.023	0.032
7	3.858	4038	315	0.039	0.045
8	4.207	3820	310	0.036	0.044
9	4.874	6690	604	0.064	0.085
10	5.755	16817	1286	0.160	0.182
11	6.191	2969	215	0.028	0.030
12	7.683	10415494	703310	99.402	99.313
13	8.729	6838	394	0.065	0.056
14	14.254	2946	167	0.028	0.024
Total		10478172	708172	100.000	100.000